ELSEVIER

Contents lists available at ScienceDirect

# Journal of Membrane Science

journal homepage: www.elsevier.com/locate/memsci





# Zeolite membrane separators for fire-safe Li-ion batteries – Effects of crystal shape and membrane pore structure

Dheeraj R.L. Murali, Fateme Banihashemi, Jerry Y.S. Lin

School for Engineering of Matter, Transport & Energy, Arizona State University, Tempe, AZ, 85287, USA

ARTICLE INFO

Keywords: Li-ion batteries Silicalite separators High concentrated electrolyte Safe battery

#### ABSTRACT

The state-of-the-art lithium-ion batteries (LIB) use carbonate-based liquid electrolytes and polymeric separators which pose safety issues including fire-hazard. The use of fire-retarding salt-concentrated electrolytes can address the safety issues of LIBs, but these electrolytes have high viscosity and low wettability with polymeric separators making it difficult to fabricate high performance LIBs with the electrolytes. Here we report development of zeolite membrane separators with tailored pore structure and surface chemistry for preparation of fire-safe LIBs using salt-concentrated electrolytes. The zeolite membrane separators are made of zeolite particles with a specific zeolite structure, Si/Al ratio, and different particle shapes, coated on cathode by a scalable blade coating method. Intermediate pore, pure silica MFI-type zeolite (silicalite) was selected as the fire-proof material for membrane separators which also offer high wettability for the fire-retarding salt-concentrated electrolyte of lithium bis (fluorosulfonyl)imide (LiFSI) in tri-methyl phosphate solvent (TMP) solvent. Two silicalite membrane separators of similar pore size but different porosity and tortuosity were coated on cathode (LiNi<sub>0.5</sub>Mn<sub>0.3</sub>Co<sub>0.2</sub>O<sub>2</sub> or NMC) using plate-shaped silicalite particles of low aspect ratio (LAR) and high aspect ratio (HAR). Both zeolite separators show significantly better wettability for the LiFSI/TMP electrolyte than the commercial polypropylene (PP) separator allowing fabrication of high-performance NMC/LiFSI-TMP/graphite cells with the noncombustible silicalite separator. The new fire-safe zeolite-membrane-based LIBs with the fire-retarding electrolyte exhibit excellent charge and discharge characteristics and cycle performance (similar to the state-of-the-art, but fire-unsafe LIBs with LiPF<sub>6</sub>-carbonate electrolyte and polymer separator). The membrane separators made of HAR plate-shaped zeolite showing low interparticle porosity and high tortuosity perform better than the membrane made of LAR zeolite particles, due to a more uniform lithium-ion flux from both interparticle pores and intraparticle zeolitic pores at the separator/anode interface.

# 1. Introduction

Lithium-ion batteries have become a preferred energy storage method and are extensively used in electronics, electric vehicles, and power storage devices [1–4]. The recent increase in the use of lithium-ion batteries has also posed a problem on the safety issue as there have been multiple reports of fire and explosion [5,6]. The majority of the safety risk associated with current LIB technology is associated with the flammable liquid electrolyte and combustible polymeric separator as the dendrites formed on the anode penetrate the low strength modulus separator, leading to short-circuiting and a thermal runaway which ignites the flammable electrolyte causes explosion/fire hazard [7–9]. For example, conventional electrolytes are mainly composed of lithium hexafluorophosphate (LiPF<sub>6</sub>) dissolved in a mixture

of cyclic carbonate (e.g., ethylene carbonate (EC)) and linear carbonates (dimethyl carbonate (DMC)) [10-12]. These organic carbonates, especially the linear carbonates, such as diethyl carbonate (DEC), dimethyl carbonate (DMC), and ethyl methyl carbonate (EMC), have high volatility and flammability, and thus present the most significant safety concern of lithium-ion batteries [13].

Solvents like trimethyl phosphate (TMP) or adiponitrile (ADN) are considered safe solvents for electrolytes because they are chemically stable and have a high boiling and flash point and low vapor pressure [14]. TMP was used as a solvent because it is a good flame retardant, has high oxidative stability and low viscosity, and can form a stable solid electrolyte interface (SEI) [15,16]. Salts such as lithium bis(trifluoromethanesulfonyl)imide (LiTFSI), lithium bis(oxalate)borate (LiBOB) and LiFSI are used to develop high salt-concentrated

E-mail address: Jerry.Lin@asu.edu (J.Y.S. Lin).

<sup>\*</sup> Corresponding author.

electrolytes (>3 M) with high lithium-ion conductivity [17]. In particular, using the salt-concentrated electrolytes consisting of LiFSI salt and TMP, without any additives or binders, have shown great improvement in the flame retardant nature as well as long cycle life. This is due to the formation of stable SEI associated with the high concentration of lithium fluoride (LiF), which also reduces the possibility of dendrite formation at the anode [16,17]. Electrolytes made of LiFSI salt have shown better thermal stability and improved performance for graphite anodes [18]. It has also shown improved lithium deposition in lithium metal batteries due to the formation of LiF rich SEI layer thus stabilizing the lithium plating and providing a solution for high voltage batteries [19]. Polymer electrolytes have also been explored for the feasibility of improving the safety and performance of the batteries [20–22].

However, these salt-concentrated electrolytes have high viscosity which greatly affects their ability to wet commercial polymeric separators as they have low surface energy and porosity. This results in slow wettability and non-uniform distribution of the electrolyte which negatively affects the battery cycle life. This also increases the battery production time [23]. Furthermore, the polymeric separators experience a large thermal shrinkage at temperatures above 90 °C. This increases the chance of an internal short circuit and thermal runaway at elevated temperatures [24]. Combining the low porosity and poor robustness of the material makes it impractical for the manufacture of fire-safe salt-concentrated electrolyte-based lithium-ion batteries. To address the issue of the thermal stability and electrolyte wettability of the polymeric separators, inorganic materials such as alumina, silica and zeolites have been studied, to improve the limitations of the commercially available polymeric separators [25].

Inorganic materials have high surface energy and exceptional mechanical stability over a wide range of temperatures. This makes them a good substitute for polymeric separators [26]. A popular approach to increase the wettability and the thermal stability of the polymeric separator is to mix the inorganic materials with a binder and coat them on the polymeric separator. Silica and alumina are a few of the popular ceramic powders used for the coating due to their low cost [27]. A novel membrane based on silicon dioxide (SiO2) and hydroxypropyl guar gum (HPG) as binder is used to coat the polymeric separator giving higher electrolyte wettability and thermal stability to the separator [28]. Another case study of using a high melting-point poly (vinyl alcohol) (PVA) binder for ceramic coating (Al<sub>2</sub>O<sub>3</sub>) of polyolefin separators has been performed to improve the thermal stability of the separator [29]. A comparative study on coating a commercial polypropylene separator with four inorganic materials, i.e., Al<sub>2</sub>O<sub>3</sub>, SiO<sub>2</sub>, ZrO<sub>2</sub> and zeolite shows that all inorganic coatings have improved thermal stability with differences in the electrical resistance but have similar cell performance as the pure polymer separator [30]. Nevertheless, the bulk of the ceramic-coated polymer separator is still organic so there is a high chance of combustion in case of thermal runaway.

Polymer free inorganic separators provide a solution to this problem. Free-standing inorganic separators have been successfully synthesized using sintered  ${\rm Al_2O_3}$  and  ${\rm SiO_2}$  powders [31,32]. However, these separators are brittle resulting in the need to make thick separators (~200  $\mu$ m) which increases the cell's internal resistance and decreases the energy density. There were further studies on decreasing the thickness of the free-standing inorganic separator. However, they require large amounts of binder with complex and chemically intensive synthesis procedure [33,34]. To address these issues, Lin and co-workers reported coating a thin (30–40  $\mu$ m) alumina [35] or silica (quartz) [36] separator directly on the electrode using the blade coating technique. These ceramic separators have shown excellent electrolyte wettability and better thermal stability and electrochemical performance of the cell, and are easily scalable providing a better choice for the commercial manufacturing process [37,38].

Recently Rafiz and Lin [39] reported using microporous zeolite (pure silica MFI type zeolite silicalite) coated on the cathode as a separator for lithium ion batteries with salt-concentrated electrolyte (such as

LiFSI/TMP). The microporous pure silica zeolite is highly wettable to the salt-concentrated electrolyte. It is much lighter than dense silica due to the presence of micropores within the particles, resulting in less reduction in energy density for lithium-ion batteries due to the use of an inorganic separator. Furthermore, the microporous zeolite separator contains both interparticle and intraparticle pores, offering more uniform Li ion flux important for maintaining uniform SEI formation. Combining the fire-retarding salt-concentrated electrolyte with a non-combustible zeolite separator leads to the construction of a fire-safe lithium-ion battery with significantly improved electrochemical performance as compared to similar batteries with separators made of dense silica particles or polypropylene [39].

In the previous work, the separator was made of particles with a low aspect ratio (close to spherical particles). It is known that the pore structure of ceramic membranes depends on the particle shape and size. Membranes made of particles with high aspec ratio have high tortuosity and are more resilient to stress. The objective of the work is to examine the effects of zeolite membrane separators consisting of zeolite particles of different aspect ratios on the performance of fire-safe lithium-ion batteries. MFI zeolite powders of low-aspect-ratio (LAR) and highaspect-ratio (HAR) plate-shaped particles were synthesized by the hydrothermal process under different conditions. The obtained zeolite powders were characterized and used to form membranes separator on the cathode by the blade-coating method. Fire-safe lithium-ion batteries were constructed with the two zeolite separators of different pore structures, and their charge-discharge curves were measured to understand the rule of the shape of zeolite particles in the electrochemical performance of the fire-safe lithium-ion batteries.

#### 2. Experiment

#### 2.1. Synthesis of zeolite powders and electrolyte

The pure silica MFI type zeolite (silicalite) was prepared using the hydrothermal synthesis method. The silicalite crystals have a pore volume of 0.19 cc/g, density of 1.76 g/cc and micropore porosity of about 33% [40,41]. Silicalite with LAR plate-shaped silicalite particles was prepared using 10 g of tetraethyl orthosilicate (Millipore Sigma), 12 g of tetra-propyl ammonium hydroxide (Millipore Sigma) and 202 g of de-ionized water were stirred in a beaker for  $\sim\!20\,h$  at room temperature till a clear solution was obtained. The solution was then heated at 130  $^{\circ}\text{C}$ for 8 h in an autoclave to obtain silicalite particles with LAR. Silicalite with HAR plate-shaped silicalite particles by a modified method from the literature [42]. To prepare HAR silicalite particles, 10 g of tetraethyl orthosilicate (Millipore Sigma), 4 g of tetra-propyl ammonium hydroxide (Millipore Sigma), and 170 g of de-ionized water were stirred in a beaker for  $\sim$ 20 h at room temperature till a clear solution was obtained. The solution was then heated at 155 °C for 10 h in an autoclave to obtain HAR plate-shaped particles.

Next, the mother liquor was decanted from the autoclave after the completion of the reaction and cooled down to the room temperature. The obtained silicalite powders were washed with de-ionized water and centrifuged at 5000 rpm (16.8 relative centrifugal force – meters) for 20 min separately. This step was repeated three to four times for silicalite powders to completely remove the organic components present in the powders post reaction. Both washed silicalite powders were then dried at 100  $^{\circ}\text{C}$  in a vacuum oven for 24 h to remove the moisture from the powders. This was followed by calcination of the powders at 600  $^{\circ}\text{C}$  in a furnace for 10 h.

The cathode used was LiNi $_{0.5}$ Mn $_{0.3}$ Co $_{0.2}$ O $_{2}$  (NMC) (94.2% active material) of thickness 45  $\mu$ m coated on aluminium foil and the anode used was graphite of thickness 50  $\mu$ m coated on copper foil (both from MTI Corporation). The lithium bis(fluorosulfonyl)imide (LiFSI) (battery grade) salt was procured from Kishida Chemical Co, Japan, and the trimethyl phosphate solvent (TMP) (reagent grade; 99.999% purity) was procured from Millipore Sigma. The required weight of LiFSI salt, and

TMP were mixed to obtain a salt-concentrated clear liquid solution of 5.3 M inside an atmosphere-controlled glovebox ( $H_2O<0.1$  ppm,  $O_2<0.1$  ppm) and the obtained solution was allowed to rest for 24 h.

#### 2.2. Coating and characterization of zeolite separators

Water based zeolite (silicalite) slurry was prepared for separator coating on the NMC cathode. For LAR or HAR plate-shaped silicalite a slurry was prepared by mixing 2 g of silicalite powder with 2 g of 5 wt% polyvinyl alcohol (PVA) aqueous solution (molecular weight: 77,000–79,000) (ICN Biomedical Inc., USA) and 1 g de-ionized water. The mixture was stirred for  $\sim\!10$  min to obtain a homogeneous slurry. The coating of the slurry on the NMC electrode was done by using a caliper-adjustable doctor blade (Gardco LLC, USA). For the coating of the silicalite separator of desired thickness, the blade gap was adjusted to 40  $\mu m$ . The prepared slurry was then dropped across one end of the electrode and then spread down the length of the electrode using the doctor blade to obtain a uniform coating. The coated separator was dried in a humidity-controlled chamber at 40 °C and 60% relative humidity for 10 h. These blade coating steps were followed to coat both LAR and HAR plate-shaped silicalite separators.

For measuring the porosity, pore size distribution and electrolyte contact angle of the zeolite membrane separators, the zeolite slurry was coated on an aluminium foil by the same blade-coating method. To measure the interparticle porosity of the coated zeolite layer, it was peeled off carefully from the aluminium foil without causing any physical damage to the separator. The interparticle porosity ( $\varepsilon$ ) of the separator was obtained from the measured bulk density (using the weight and dimensional volume of the zeolite separator) and zeolite particle density as [43]:

$$\epsilon = 1 - \frac{\rho_{bulk}}{\rho_{particle}} \tag{1}$$

The zeolite layer on the aluminium foil was cut into small pieces and used to measure interparticle pore size using a mercury porosimeter (Micrometrics Auto Pore V, USA) performed at both the high-pressure mode and low-pressure mode to detect pore sizes ranging from nanometer to micrometer dimensions.

The morphology and phase structure of prepared silicalite powders and separators coated on the NMC cathode were respectively observed using scanning electron microscopy (Philips, USA, FEI XL-30, with sample sputter-coated with gold) and X-ray diffraction patterns were obtained (Bruker AXS-D8, Cu Ka radiation, USA). The electrolyte contact angle measurement was done to both silicalite particles coated on the aluminium foil and PP separator by dropping the 5.3 M LiFSI/TMP electrolyte on a DSA-25 Drop Shape Analyzer (Kruss, USA) and the images were recorded at intervals of 1 s.

# 2.3. Cell assembly and electrochemical characterization

The NMC electrodes coated with silicalite separators were cut into 16 mm diameter discs using the disc cutter (MTI Corporation) and the cut discs were kept in a vacuum oven at 70 °C for 12 h. The obtained discs were then immediately placed inside an argon-filled glovebox (Innovative Technology Inc., USA) and kept in it for a period of 24 h to remove any traces of atmospheric gases or moisture in the electrodesupported separator disks. The coin cells of CR2032 type (X2 Labwares, Singapore) were assembled inside the glovebox. The silicalite coated NMC discs of 16 mm in diameter were first placed inside the bottom case of the coin cell and the prepared 5.3 M LiFSI/TMP electrolyte of  $150\,\mu l$  was pipetted out onto the surface of the silicalite coated NMC cathode. Graphite anode of 16 mm was then placed on top of the separator surface and followed by two spacers and one spring. Finally, the top case of the coin cell was placed to enclose the coin cell. The coin cell was sealed by crimping at 400 psi. This procedure was used to construct coin cells for both electrodes coated with LAR and HAR plateshaped silicalite separators.

The constructed coin cells were then removed from the glovebox and the charge-discharge characteristics of the cells were tested using a battery testing system (BTS3000) (Neware Co, Shenzen, China). The cells were cycled using the standard CC–CV (constant current– constant voltage) method where the minimum and maximum potential for testing were respectively 2.0 V and 4.2 V. The cells prepared using both LAR and HAR plate-shaped silicalite separators were first tested at 0.2C-rate (0.708 mA) for 100 cycles to examine the cycle life performance of the cells. Subsequently, the cells were cycled at higher C-rates of 0.5C, 1C and 2C to test the rate capability of the cells using LAR and HAR plate-shaped silicalite separators.

Electrochemical impedance spectroscopy (EIS) measurements of the assembled cells were conducted using a PARSTAT 2263 EIS station (Princeton Applied Research, USA) in the AC mode to analyse the internal resistance of the cells. The Nyquist plots were obtained for the assembled cells (at 100% SOC) by electrochemical impedance spectroscopy (EIS) (PARSTAT 2263 EIS station, Princeton Applied Research, USA) in a frequency range of 100 kHz to 10 mHz and an AC amplitude of 10 mV rms.

#### 3. Results and discussion

# 3.1. Characteristics of zeolite membrane separators

Pure silica MFI-type zeolite (silicalite) powders of LAR and HAR plate-shaped particles were synthesized by the hydrothermal method from tetraethyl orthosilicate with tetra-propyl ammonium hydroxide as an organic template. Fig. 1 shows SEM micrographs and XRD patterns of the two silicalite powders. Both powders exhibit facet morphology with similar thickness, but the HAR particles have much larger width and length as compared to the LAR particles, as summarized in Table 1. The aspect ratio is defined as ratio of the length to the thickness which is about 10–40 for the HAR particles and about 2–4 for the LAR particles. The XRD patterns for these two samples are typical of MFI zeolite [44], showing no preferential orientation, due to the random packing of these particles in the samples for XRD analysis.

The silicalite powders were mixed into an aqueous solution using polyvinyl alcohol (PVA) as the binder and the slurry was coated on the NMC cathode to obtain a coating of the wet silicalite separator of 40  $\mu m$  thickness. The PVA added to the slurry mixture was reduced to a minimum level (2 wt%) so to avoid it affecting the electrochemical performance of the cell.

Fig. 2 shows the SEM images of the surface and cross-sectional views of the LAR and HAR plate-shaped silicalite separator layers coated on the NMC cathode. The surface image shows the morphology of silicalite particles of LAR and HAR plate-shaped particles, similar to the corresponding powder shown in Fig. 1. The cross-sectional SEM images show three layers of metal backing, NMC and silicalite separator. The thickness of the LAR and HAR plate-shaped silicalite separator layers is about 35 and 30  $\mu m$ , respectively, shrunk from 40  $\mu m$  in thickness for the ascoated wet separators due to drying process in the humid chamber followed by drying in a vacuum oven. The HAR plate-shaped particles shrunk more than LAR particles.

Fig. 3 shows XRD patterns of the silicalite separator coated on the NMC cathode before and after compression at 400 psi, and SEM micrograph of the surface of the silicalite separator after compression at 400 psi, made from the LAR and HAR plate-shaped silicalite powders. Similar XRD patterns and micrograph for silicalite separator on the NMC cathode made from HAR plate-shaped silicalite powder are given in Fig. 4. Comparison of the SEM micrographs of the surface of the silicalite separators before (Fig. 2) and after (Fig. 3b and 4b) compression shows no observable difference in surface morphology. For separator made from LAR particles, the XRD patterns show no difference indicating compression does not change the orientation of the particles. However, for HAR plate-shaped silicalite separator the XRD patterns show that

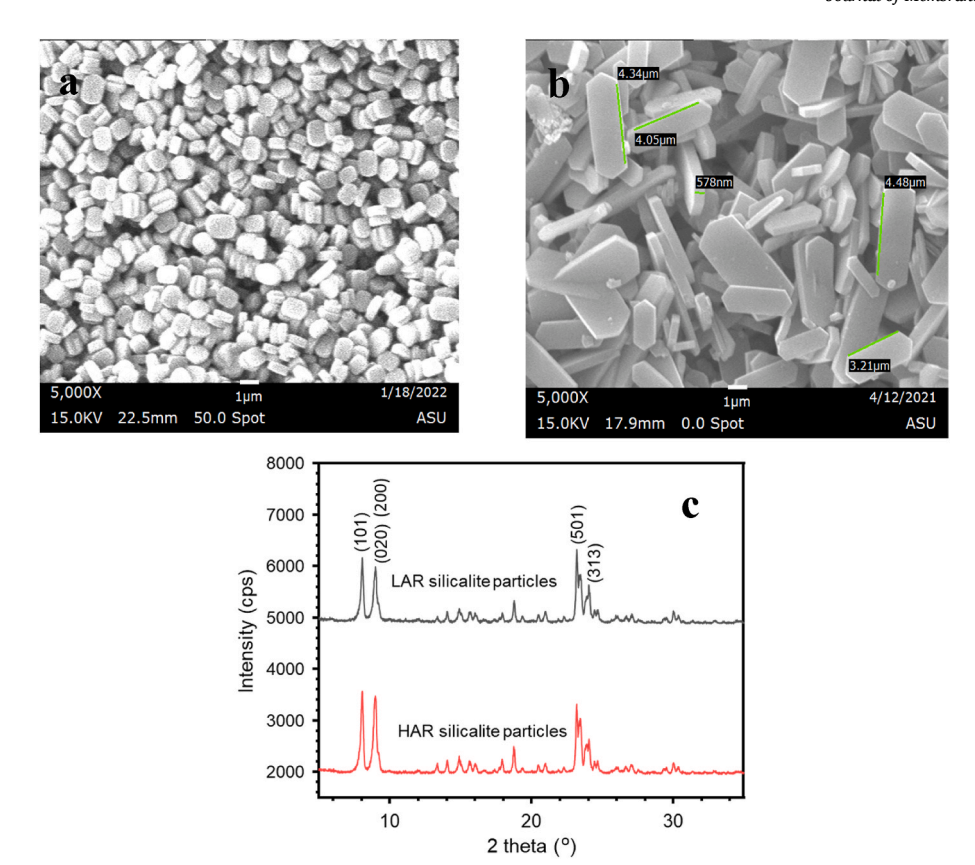


Fig. 1. SEM micrographs of the LAR(a) and HAR (b) plate-shaped MFI zeolite (silicalite) synthesized in this work and corresponding XRD patterns of powders of the zeolite (c).

**Table 1**Characteristic lengths of the zeolite (silicalite) particles and pore structure of the corresponding zeolite membrane separators.

Plate-shaped Zeolite	Typical particle dimension			Separator		
	Thickness (μm)	Width (μm)	Length (μm)	Average pore diameter (μm)	Interparticle Porosity (%)	
LAR silicalite	0.2-0.5	1–1.5	1–1.5	0.4	72	
HAR silicalite	0.2-0.5	2–3	4–8	0.4	59	

compression results in an enhancement in (020) plane (b-axis) peak intensity. For HAR particles, the large surface is normal to b-axis straight channels for MFI zeolite [45]. This suggests that compression enhances the orientation of the HAR plate-shaped particles along the flat plane of the silicalite crystals. Since the compression force acts in the direction normal to the cathode surface, the compression reorients the HAR plate-shaped silicalite particles with large planes aligned parallel to the surface of the NMC electrode. Thus, the b-axis straight intracrystalline pores are better aligned with the lithium-ion flux direction.

Silicalite powders were coated from the same slurries by the blade coating method on aluminium foil for the analysis of porosity and pore size distribution of the silicalite separators. Fig. 5(a) and (b) shows pore size distributions of the LAR and HAR plate-shaped silicalite separator respectively. Both membrane separators have essentially the same interparticle pore size distribution. The average pore size and porosity for the LAR and HAR plate-shaped particle silicalite separator are listed in Table 1. The HAR plate-shaped particle separator has lower porosity and essentially the same pore size as compared to the LAR particle separator. These results can be explained by the structure of the pores illustrated in Fig. 5(c) and (d). The LAR and HAR plate-shaped silicalite particles have the same thickness, which determines the interparticle pore size. The HAR plate-shaped silicalite separator layer shows more compact packing and tortuous interparticle pathway than the LAR

silicalite separator. Since Li ion may transport through intracrystalline (intraparticle) pores in the direction indicated in Fig. 5 and HAR plate-shaped silicalite has straight intraparticle crystalline pores aligned with Li ion flux direction, the contribution of the Li ion flux through intraparticle pores of the HAR silicalite separator will be larger than that of the LAR silicalite separator. Such differences in pore structure and particle orientation of the separator will impact the performance of the batteries made with these separators.

A single sessile drop wettability test was performed to show the wettability of the prepared silicalite separators towards salt-concentrated electrolyte and compare them with the commercially obtained polypropylene separator (PP-2500, Celgard). The prepared liquid salt-concentrated 5.3 M LiFSI/TMP electrolyte was dropped against the separators to measure the contact angle. Fig. 6 shows the contact angle measurements of the silicalite and PP separators as a function of time. Both silicalite separators have much lower contact angle than the PP separator due to the hydrophobic nature of the pure silica MFI-type zeolite and the presence of intracrystalline micropores in the zeolite particles [46]. The HAR plate-shaped silicalite separator has a lower contact angle than the LAR silicalite separator suggesting that the HAR plate-shaped silicalite is more wettable for the salt-concentrated electrolyte. This translates to fast loading and more uniform filling of the high salt-concentrated electrolyte in the pores of the zeolite separator, in

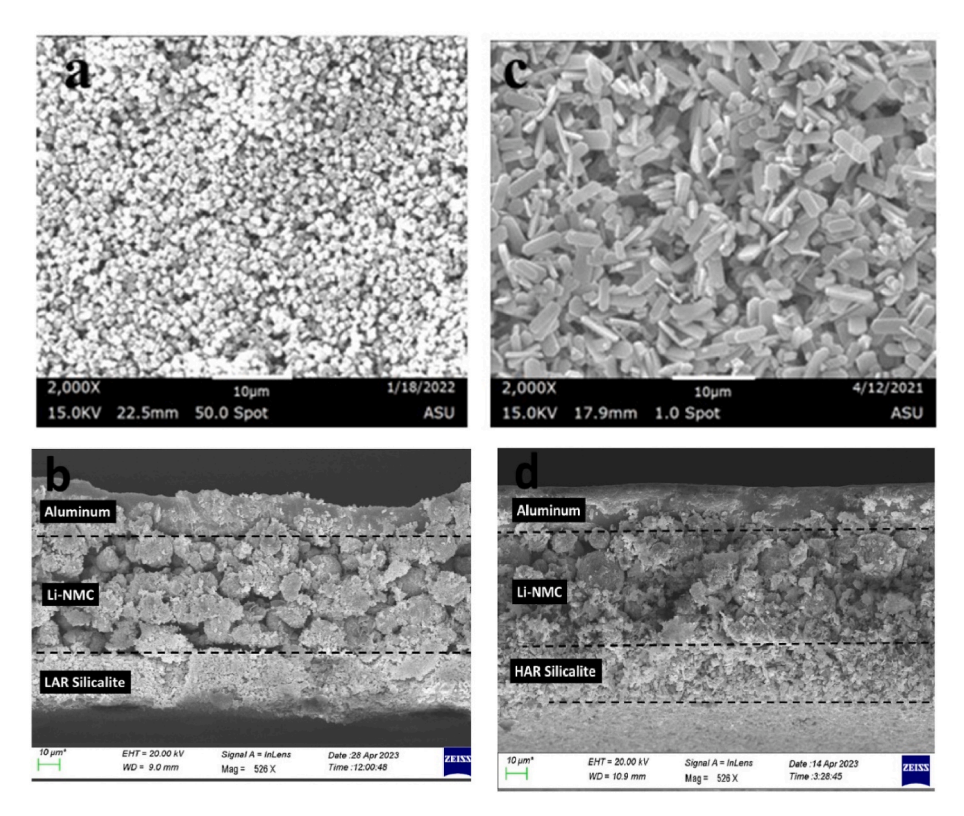


Fig. 2. Surface (top) and cross-sectional (bottom) SEM micrographs of the LAR (a and b) and the HAR (c and d) plate-shaped silicalite coated NMC cathode.

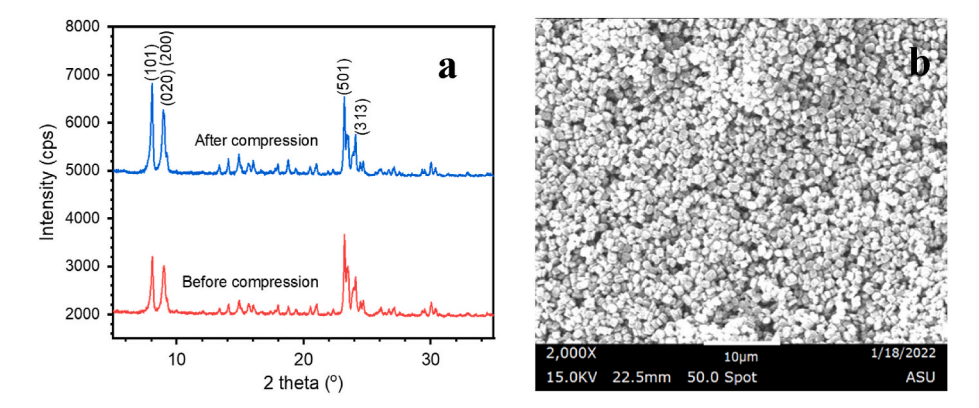


Fig. 3. (a) XRD patterns of the LAR silicalite separator coated on NMC cathode before and after compression, (b) SEM micrograph of the LAR silicalite separator after compression [before compression is given in Fig. 2(a)].

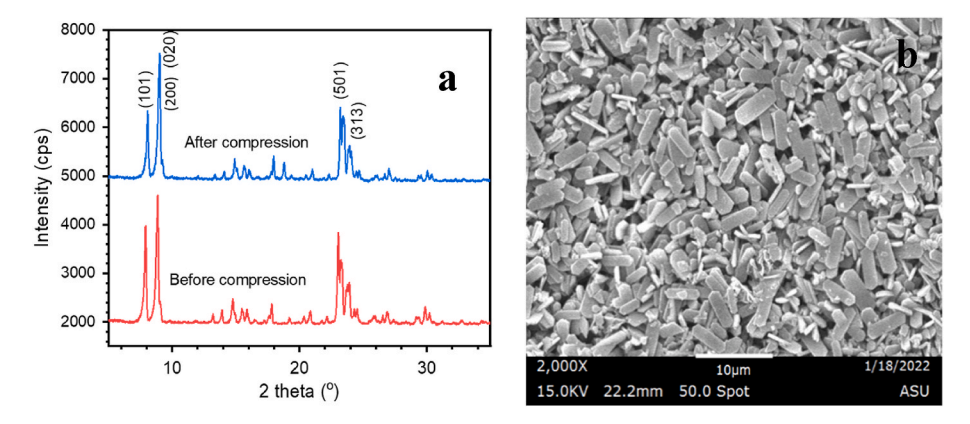


Fig. 4. (a) XRD patterns of the HAR plate-shaped silicalite separator coated on NMC cathode before and after compression, (b) SEM micrograph of the HAR silicalite separator after compression [before compression is given in Fig. 2(b)].

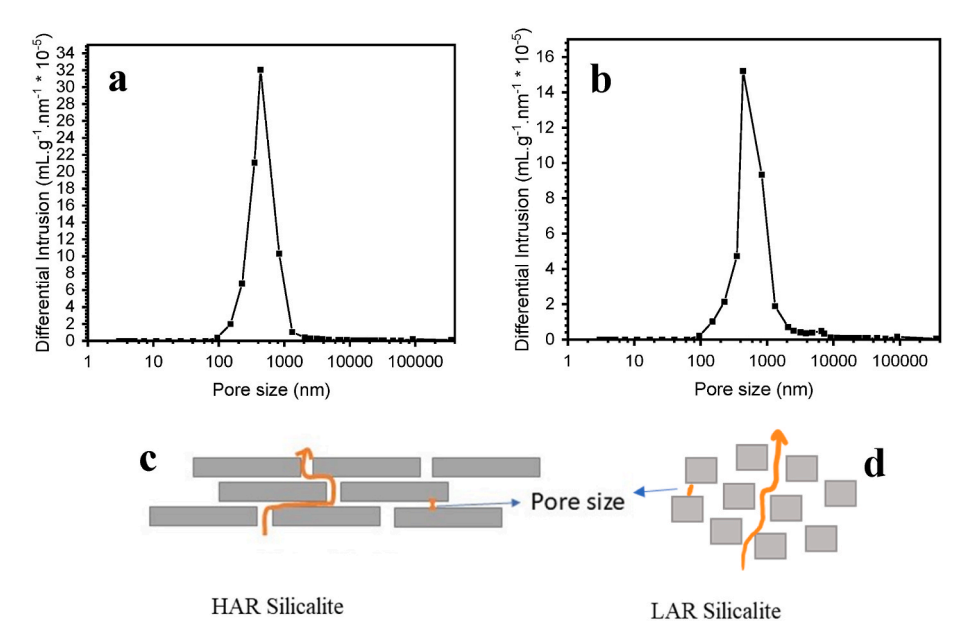


Fig. 5. Pore size distribution of the HAR plate-shaped silicalite separator (a) and the LAR silicalite separator (b) measured by Hg porosimetry, and illustration of the pore structure of the HAR silicalite separator (c) and the LAR silicalite separator (d) with arrows indicating interparticle transport pathway for Li ions.

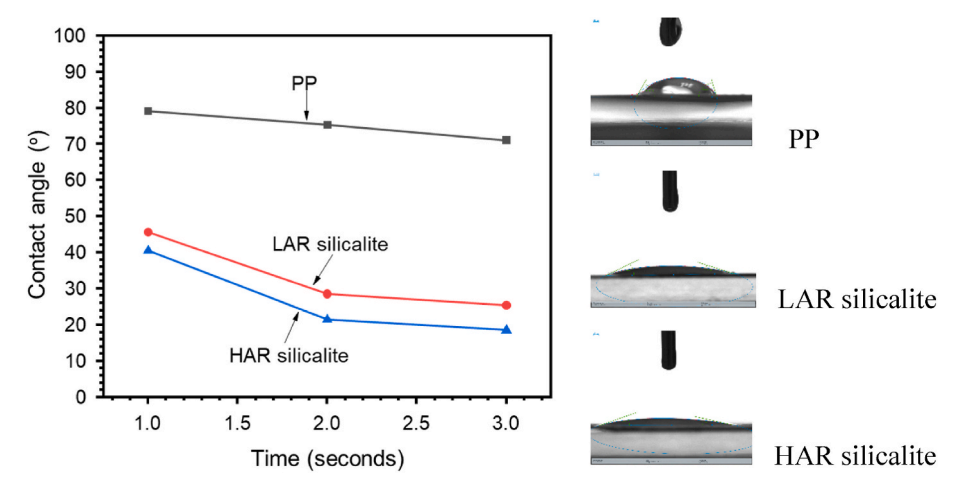


Fig. 6. Change in the contact angle with time for PP, HAR and LAR silicalite membranes showing the wettability of LiFSI/TMP electrolyte, and photo of contact angle at 3 s.

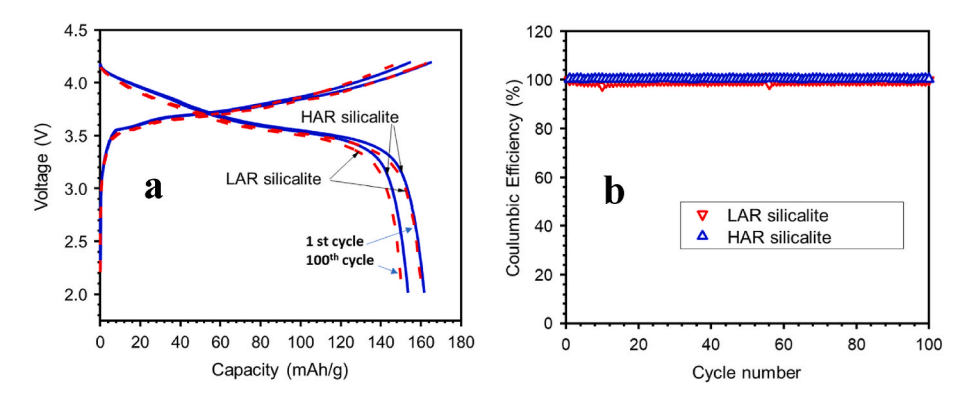


Fig. 7. (a) CC-CV curves for charge and discharge cycles of 1st and 100th cycle for the full-cells with LAR and HAR plate-shaped silicalite separators at 0.2C and (b) Coulombic efficiency of the first 100 cycles for the full cells with LAR and HAR plate-shaped silicalite separators at 0.2C.

particular of the HAR plate-shaped zeolite, enabling the good electrochemical performance of the LIBs made with the high salt-concentrated electrolyte [36].

# 3.2. Electrochemical performance of the NMC/graphite cells with zeolite separators

Full NMC/graphite cells were constructed using NMC coated with LAR and HAR plate-shaped silicalite powders prepared in this work as separators filled with 5.3 M LiFSI/TMP electrolyte and cycled using the CC-CV charge-discharge method. Fig. 7(a) shows the charge and discharge curves of the 1st cycle and the 100th cycle for both separators made of LAR and HAR plate-shaped silicalite particles at 0.2C-rate. Both cells show typical charge-discharge curves for NMC/graphite full cells with a discharge capacity of about 160 mAh/g. In our previous study, full cells constructed using NMC/graphite as electrodes with LAR silicalite, dense (quartz) silica and PP-2500 separators filled with 5.3 M LiFSI/TMP electrolyte were tested for their electrochemical performance and the LAR silicalite separator has shown significantly better electrical performance in terms of capacity retention and rate capability than cells with dense silica and PP separators [39]. The cell with the LAR silicalite separator prepared in the present work exhibits the same charge and discharge characteristics as the same cell with the LAR silicalite separator prepared by the previous researcher [39], verifying the reproducibility of the zeolite separator technology. In the present study, both cells showed essentially 100% coulombic efficiency for 100 cycles as shown in Fig. 7(b). However, the cell with the HAR silicalite separator has a higher capacity, better capacity retention and slightly larger coulombic efficiency compared to the cell with the LAR silicalite separator. This suggests a more uniform and thin SEI layer formation for the cell with the HAR silicalite separator as compared to the LAR silicalite separator resulting in fewer loss of active lithium ions and better coulombic efficiency.

To further understand the cell performance, these cells with the same configurations were again tested using the electrochemical impedance spectrometer (EIS) and the Nyquist plots for the full cells were obtained as shown in Fig. 8. The Nyquist plots for the fully charged cells give the impedance parameters of the ohmic resistance, SEI resistance and charge transfer resistance after the data is fitted to the equivalent circuit using EC-Lab software, which are listed in Table 2 along with the thickness and geometric factor of the silicalite separators. The ohmic resistance of the cell represents the resistance of the separator filled with

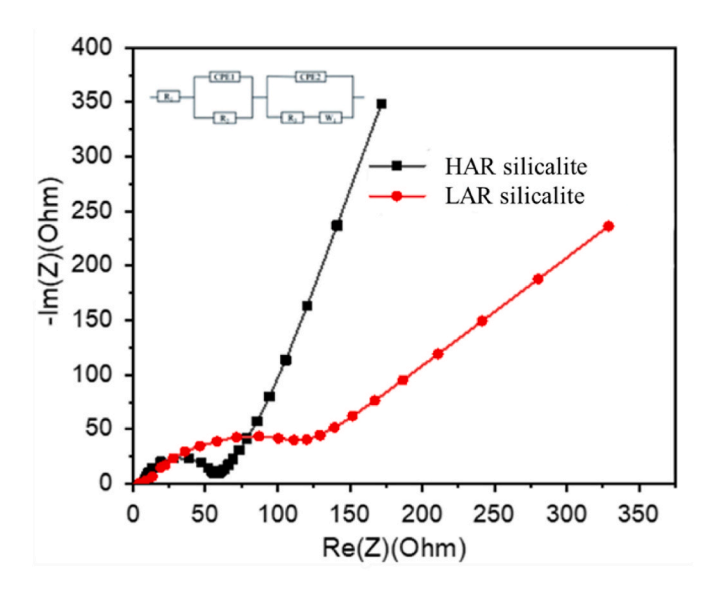


Fig. 8. Fitted Nyquist impedance plots for full cells of LAR and HAR plate-shaped silicalite separators.

**Table 2**Values of fitted impedance parameters for full cells of the LAR and HAR plate-shaped silicalite membrane separators.

Separator	Thickness (L) (µm)	Normalized thickness (L/ $\epsilon$ ) ( $\mu$ m)	R <sub>ohm</sub> (Ω)	R <sub>SEI</sub> (Ω)	R <sub>ct</sub> (Ω)
LAR silicalite	35	48.0	4.41	71.3	131
HAR silicalite	30	50.8	7.83	45.0	66.6

the electrolyte, which is related to the effective lithium ion conductivity of the electrolyte in the pores of the separator ( $\sigma$ ) and pore structure of the separator (separator area A, thickness L, porosity  $\epsilon$ , pore tortuosity  $\tau$ ) as [47]:

$$R = \frac{L}{\varepsilon A} \frac{\tau}{\sigma} \tag{2}$$

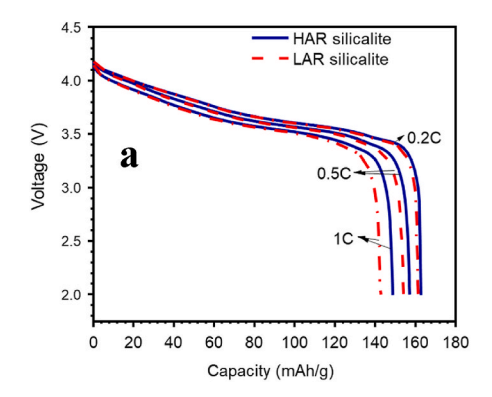
The ohmic resistance of the HAR plate-shaped silicalite separator  $(7.83 \Omega)$  is about 1.8 times that of the LAR silicalite separator  $(4.41 \Omega)$ . For both separators (L/ $\epsilon$ ) is similar (see Table 2) and A is the same. This means that the ratio of  $(\tau/\sigma)$  for the HAR plate-shaped silicalite separator is larger than that for the LAR silicalite separator. Since the HAR plate-shaped silicalite separator is more wettable to the electrolyte than the LAR silicalite as shown in Fig. 6, the effective conductivity for the former is expected to be larger than the latter. Thus, this result suggests that the tortuosity factor for the HAR plate-shape silicalite separator will be at least 1.8 times larger than that for the LAR silicalite separator, consistent with a recent study showing tortuosity increases with decreasing sphericity of the particles [48]. The cell with the HAR silicalite separator also has lower SEI and charger transfer resistance than that with the LAR silicalite separator, as shown in Table 2, indicating the positive impact of the HAR plate-shape of zeolite particles on improving cell performance.

Fig. 9(a) shows the discharge curve for the 1st cycle of the cells with the LAR and HAR plate silicalite separators at 0.2C, 0.5C, 1C and 2C. We can see that as the C-rate increases there is a significant difference in the discharge curves between LAR and HAR plate-shaped silicalite separators. HAR plate-shaped silicalite separators. HAR plate-shaped silicalite separators shows much better discharge characteristics at a high C-rate than the LAR silicalite.

Different from the separator made of dense silica particles containing only interparticle pores, the zeolite (silicalite) separator includes both interparticle pores with characteristics shown in Table 1, and intraparticle crystalline zeolite pores. MFI zeolites have straight zeolitic pores in b-axis and zig-zag pores in a-axis, with a pore diameter of around 0.55 nm. Cells with the LAR microporous pure silica zeolite (silicalite) separator perform better than the cells with dense silica because in the former Li-ions can transport through both interparticle pores and intraparticle crystalline zeolitic pores filled with electrolyte [49,50], resulting in a more uniform Li flux and distribution at the separator/anode interface. To confirm qualitatively Li-ion flux through intraparticle pores of silicalile, Li-ion conductivity ( $\sigma_m$ ) for electrolyte filled free-standing separator films made of (a) plate-shaped HAR silicalite (average aspect ratio  $\sim$  25) and (b) plate-shaped  $\gamma$ -Al<sub>2</sub>O<sub>3</sub> particle without intraparticle pores with a significantly lower aspect ratio (~6) [51] were measured. The tortuosity of the separator was calculated from the measured conductivity data and the intrinsic Li-ion conductivity of liquid electrolyte ( $\sigma$ ) and interparticle porosity of separator ( $\epsilon$ ) by

$$\tau = \frac{\sigma \cdot \varepsilon}{\sigma_{m}} \tag{3}$$

The determined tortuosity for the HAR zeolite separator (6.31) is slightly smaller than that for  $\gamma$ -Al<sub>2</sub>O<sub>3</sub> membrane separator (6.95). From the huge difference in the aspect ratio of particle between the zeolite and  $\gamma$ -Al<sub>2</sub>O<sub>3</sub> (~25 vs ~6), one should expect much higher tortuosity for the zeolite separator than the alumina one as discussed above. The results indicate that the measured Li-ion conductivity ( $\sigma$ <sub>m</sub>) for the electrolyte



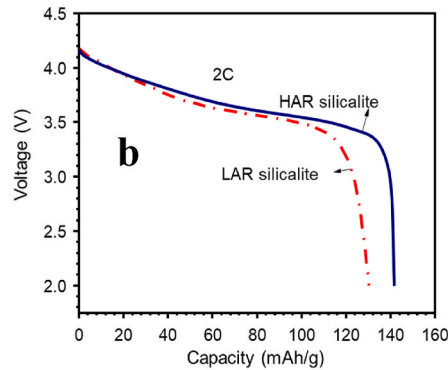


Fig. 9. CC-CV discharge curves of 1st cycle for the cells with HAR and LAR silicalite separator (a) at 0.2C, 0.5C, 1C and (b) at 2C-rate.

filled zeolite separator is much higher than that contributed by interparticle Li-ion flux, suggesting a significant contribution of Li-ion flux through zeolite intraparticle pores.

For the HAR plate-shaped silicalite separator, the particles are arranged such that the straight zeolitic pores are aligned with the Li-ion flux direction, and thus may offer more uniform Li-ion flux at the separator-anode interface than the LAR silicalite separator. It is known that a more uniform Li-ion flux at the separate-anode interface provides a more uniform and robust solid-electrolyte interface (SEI) and better availability of the Li-ions at the lithium metal anode, resulting in a significantly enhanced performance of lithium-metal battery cells [52, 531. For lithium-ion batteries, Li-ion transport through the intraparticle micropores of MFI zeolite crystals may also result in a more uniform and thin SEI layer and fewer loss of active lithium ions, and hence better capacity retention and columbic efficiency for the cells with the HAR plate-shaped separator than the cells with the LAR silicalite separator. Similarly, as the C-rate increases the Li-ions in the separator tend to transport more through intraparticle micropores of the HAR plate-shaped silicalite particles rather than the inter-particle porous pathway which is more tortuous. This in turn provides uniform Li-ion flux along the anode resulting in a uniform and thin SEI layer. Li-ions tend to diffuse along the interparticle pathway for the LAR silicalite separator as they as less tortuous which results in less-uniform Li-ion flux and SEI layer. This is even more apparent at a high C-rate (2C) as shown in Fig. 9(b).

For LIB cells with polymer separators thermal runaway is usually accompanied with a rise in temperature resulting in shrinkage of the separator and eventually short circuit of the cell [54,55]. In the case of silicalite separators they are structurally stable even at high temperatures. To study the stability of the separators and their electrochemical performance, two full cells were assembled using the LAR and HAR plate-shaped silicalite separators and the high salt-concentrated LiF-SI/TMP electrolyte and cycled at 0.2C at different temperatures. The cells were first cycled at 25  $^{\circ}$ C while recording the cell performance and the temperature was decreased to 0  $^{\circ}$ C in a stepwise manner and the cells were allowed to cycle for cycles at each temperature. The temperature was then increased from 0  $^{\circ}$ C to 70  $^{\circ}$ C, and the capacity retention was plotted against the cycle number as shown in Fig. 10.

As the temperature decreases from 25 °C to 0 °C, the electrolyte conductivity and diffusivity decrease due to the increase in the viscosity of the electrolyte as shown in the studies by different research groups [56–59]. This leads to increase in the ohmic polarization and in turn a reduction in the capacity with decreasing temperature as seen in both separators [60]. However, the LAR silicalite separator shows better performance as compared to the HAR silicalite separator due to its higher porosity and lower tortuosity which facilitate electrolyte diffusion. As the temperature increases from 0 °C to 70 °C the HAR plate-shaped silicalite separator shows better performance due to its lower SEI and charge transfer resistances. It should be noted that MFI

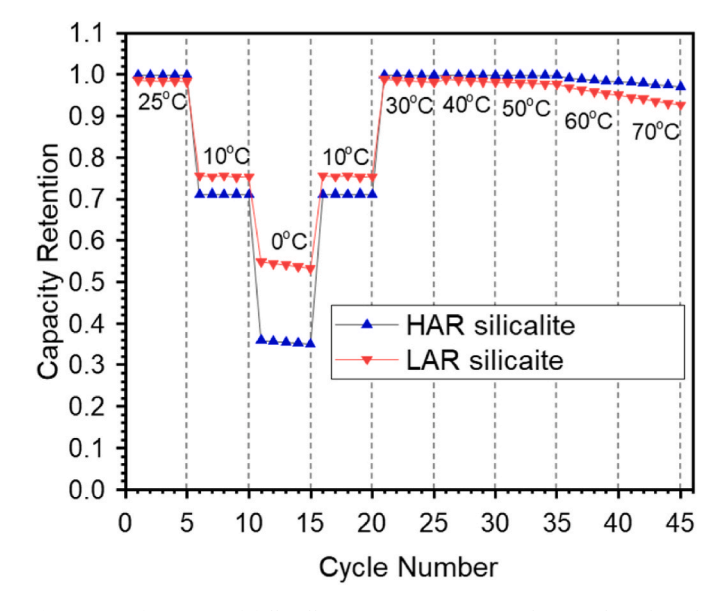


Fig. 10. Performance of full cells at 0.2C using LAR and HAR plate-shaped silicalite separators at different temperatures.

zeolite has a small, but negative thermal expansion coefficient  $(-0.0003\%^{\circ}C)$ , with negative sign meaning that it shrinks with increasing temperature) [61]. Thus, zeolite separator essentially does not change in the temperature range studied in the work.

# 4. Conclusions

Pure silica MFI type zeolite (silicalite) separators of the same interparticle pore size but different porosity and tortuosity can be bladecoated on LiNi<sub>0.5</sub>Mn<sub>0.3</sub>Co<sub>0.2</sub>O<sub>2</sub> (NMC) cathode using silicalite powders of low-aspect-ratio (LAR) or high-aspect-ratio (HAR). The zeolite separators exhibit significantly higher wettability towards the saltconcentrated LiFSI/TMP electrolyte than the commercial polypropylene separator, enabling the fabrication of fire-safe NMC/graphite cells with non-combustible zeolite separator and fire-retarding LiFSI/ TMP electrolyte. The fire-safe cells show good charge and discharge characteristics and cycle performance. The HAR plate-shaped silicalite separator has better capacity retention and rate capability with lower SEI and charge transfer resistances than the LAR silicalite separator due possibly to more uniform Li-ion flux from both interparticle pores and intrazeolitic pores at the separator/anode interface. The HAR plateshaped silicalite separator also shows better performance at higher temperatures as compared to the LAR silicalite separator, offering potential to develop fire-safe lithium-ion batteries with better cycle life, rate capability and non-flammablility.

#### Author statement

Dheeraj R.L. Murali: Investigation, Formal analysis, Data curation, Methodology, Writing-original draft preparation, Fateme Banihashemi: Formal analysis, Data curation, Writing-original draft preparation, Jerry Y.S. Lin: Methodology, Formal analysis, Resources, Supervision, Project administration, Funding acquisition, Writing-review & editing.

#### Declaration of competing interest

The authors declare the following financial interests/personal relationships which may be considered as potential competing interests:

Arizona State University has entered into a license agreement with Safe-Li LLC on development of zeolite membrane separator technology for safe-lithium ion batteries. JYSL is a co-founder and chief scientist of Safe-Li LLC.

#### Data availability

Data will be made available on request.

#### Acknowledgment

We acknowledge the support of the National Science Foundation (CBET-2031087 CBET-2200204) on zeolite membrane research from which this project benefit and ASU Catalysis Fund for supporting the work.

#### References

- [1] K.W. Beard, Linden's Handbook of Batteries, McGraw-Hill Education, 2019.
- [2] D. Deng, Li-ion batteries: basics, progress, and challenges, Energy Sci. Eng. 3 (2015) 385–418.
- [3] R. Marom, S.F. Amalraj, N. Leifer, D. Jacob, D. Aurbach, A review of advanced and practical lithium battery materials, J. Mater. Chem. 21 (2011) 9938–9954.
- [4] B. Scrosati, Recent advances in lithium ion battery materials, Electrochim. Acta 45 (2000) 2461–2466.
- [5] Q. Wang, P. Ping, X. Zhao, G. Chu, J. Sun, C. Chen, Thermal runaway caused fire and explosion of lithium ion battery, J. Power Sources 208 (2012) 210–224.
- [6] Y. Zhu, J. Xie, A. Pei, B. Liu, Y. Wu, D. Lin, Y. Cui, Fast lithium growth and short circuit induced by localized-temperature hotspots in lithium batteries, Nat. Commun. 10 (2019) 1–7.
- [7] D. Ren, X. Feng, L. Lu, M. Ouyang, S. Zheng, J. Li, X. He, An electrochemical-thermal coupled overcharge-to-thermal-runaway model for lithium ion battery, J. Power Sources 364 (2017) 328–340.
- [8] T. Wu, H. Chen, Q. Wang, J. Sun, Comparison analysis on the thermal runaway of lithium-ion battery under two heating modes, J. Hazard Mater. 344 (2018) 733–741.
- [9] X. Feng, J. Sun, M. Ouyang, F. Wang, X. He, L. Lu, H. Peng, Characterization of penetration induced thermal runaway propagation process within a large format lithium ion battery module, J. Power Sources 275 (2015) 261–273.
- [10] N. Chawla, N. Bharti, S. Singh, Recent advances in non-flammable electrolytes for safer lithium-ion batteries, Batteries 5 (2019) 19.
- [11] L. Jiang, Q. Wang, K. Li, P. Ping, L. Jiang, J. Sun, A self-cooling and flame-retardant electrolyte for safer lithium ion batteries, Sustain. Energy Fuels 2 (2018) 1323–1331.
- [12] T. Gao, B. Wang, L. Wang, G. Liu, F. Wang, H. Luo, D. Wang, LiAlCl4-3SO2 as a high conductive, non-flammable and inorganic non-aqueous liquid electrolyte for lithium ion batteries, Electrochim. Acta 286 (2018) 77–85.
- [13] P. Shi, S. Fang, J. Huang, D. Luo, L. Yang, S.I. Hirano, A novel mixture of lithium bis (oxalato) borate, gamma-butyrolactone and non-flammable hydrofluoroether as a safe electrolyte for advanced lithium ion batteries, J. Mater. Chem. 5 (2017) 19982–19990.
- [14] D. Farhat, F. Ghamouss, J. Maibach, K. Edström, D. Lemordant, Adiponitrile-lithium bis (trimethylsulfonyl) imide solutions as alkyl carbonate-free electrolytes for Li4Ti5O12 (LTO)/LiNi1/3Co1/3Mn1/3O2 (NMC) Li-ion batteries, ChemPhysChem 18 (2017) 1333–1344.
- [15] X. Wang, C. Yamada, H. Naito, G. Segami, K. Kibe, High-concentration trimethyl phosphate-based nonflammable electrolytes with improved charge-discharge performance of a graphite anode for lithium-ion cells, J. Electrochem. Soc. 153 (2005) 135.
- [16] J. Wang, Y. Yamada, K. Sodeyama, E. Watanabe, K. Takada, Y. Tateyama, A. Yamada, Fire-extinguishing organic electrolytes for safe batteries, Nat. Energy 3 (2018) 22–29.
- [17] P. Shi, H. Zheng, X. Liang, Y. Sun, S. Cheng, C. Chen, H. Xiang, A highly concentrated phosphate-based electrolyte for high-safety rechargeable lithium batteries, Chem. Commun. 54 (2018) 4453–4456.

- [18] S.-J. Kang, K. Park, S.-H. Park, H. Lee, Unraveling the role of LiFSI electrolyte in the superior performance of graphite anodes for Li-ion batteries, Electrochim. Acta 259 (2018) 949–954.
- [19] G. Yang, Y. Li, S. Liu, S. Zhang, Z. Wang, L. Chen, LiFSI to improve lithium deposition in carbonate electrolyte, Energy Storage Mater. 23 (2019) 350–357.
- [20] T.F. Miller III, Z.-G. Wang, G.W. Coates, N.P. Balsara, Designing polymer electrolytes for safe and high capacity rechargeable lithium batteries, Acc. Chem. Res. 50 (2017) 590–593.
- [21] J. Zhang, B. Sun, X. Huang, S. Chen, G. Wang, Honeycomb-like porous gel polymer electrolyte membrane for lithium ion batteries with enhanced safety, Sci. Rep. 4 (2014) 6007.
- [22] D. Zhou, D. Shanmukaraj, A. Tkacheva, M. Armand, G. Wang, Polymer electrolytes for lithium-based batteries: advances and prospects, Chem 5 (2019) 2326–2352.
- [23] M.H. Ryou, Y.M. Lee, J.K. Park, J.W. Choi, Mussel-inspired polydopamine-treated polyethylene separators for high-power Li-ion batteries, Adv. Mater. 23 (2011) 3066–3070.
- [24] J. Allen, Review of polymers in the prevention of thermal runaway in lithium-ion batteries, Energy Rep. 6 (2020) 217–224.
- [25] C.L. Eggen, P.M. McAfee, Y. Jin, Y.S. Lin, Surface roughness and chemical properties of porous inorganic films, Thin Solid Films 591 (2015) 111–118.
- [26] L. Yu, J. Miao, Y. Jin, J. Lin, A comparative study on polypropylene separators coated with different inorganic materials for lithium-ion batteries, Front. Chem. Sci. Eng. 11 (2017) 346–352.
- [27] N. Burriesci, M.L. Crisafulli, N. Giordano, J.C.J. Bart, G. Polizzotti, Hydrothermal synthesis of zeolites from low-cost natural silica-alumina sources, Zeolites 4 (1984) 384–388
- [28] D.V. Carvalho, N. Loeffler, G.T. Kim, S. Passerini, High temperature stable separator for lithium batteries based on SiO2 and hydroxypropyl guar gum, Membranes 5 (2015) 632–645.
- [29] L. Yu, Y. Jin, Y.S. Lin, Ceramic coated polypropylene separators for lithium-ion batteries with improved safety: effects of high melting point organic binder, RSC Adv. 6 (2016) 40002–40009.
- [30] L. Yu, J. Miao, Y. Jin, J. Lin, A comparative study on polypropylene separators coated with different inorganic materials for lithium-ion batteries, Front. Chem. Sci. Eng. 11 (2017) 346–352.
- [31] H. Xiang, J. Chen, Z. Li, H. Wang, An inorganic membrane as a separator for lithium-ion battery, J. Power Sources 196 (2011) 8651–8655.
- [32] J. Chen, S. Wang, D. Cai, H. Wang, Porous SiO2 as a separator to improve the electrochemical performance of spinel LiMn2O4 cathode, J. Membr. Sci. 449 (2014) 169–175.
- [33] M. He, X. Zhang, K. Jiang, J. Wang, Y. Wang, Pure inorganic separator for lithium ion batteries, ACS Appl. Mater. Interfaces 7 (2015) 738–742.
- [34] M. Raja, N. Angulakshmi, S. Thomas, T.P. Kumar, A.M. Stephan, Thin, flexible and thermally stable ceramic membranes as separator for lithium-ion batteries, J. Membr. Sci. 471 (2014) 103–109.
- [35] G. Sharma, Y. Jin, Y.S. Lin, Lithium ion batteries with alumina separator for improved safety, J. Electrochem. Soc. 164 (2017) 1184.
- [36] K. Rafiz, Y. Jin, Y.S. Lin, Performance of electrode-supported silica membrane separators in lithium-ion batteries, Sustain. Energy Fuels 4 (2020) 1254–1264.
- [37] S.S. Zhang, A review on the separators of liquid electrolyte Li-ion batteries, J. Power Sources 164 (2007) 351–364.
- [38] Y. Xie, H. Zou, H. Xiang, R. Xia, D. Liang, P. Shi, H. Wang, Enhancement on the wettability of lithium battery separator toward nonaqueous electrolytes, J. Membr. Sci. 503 (2016) 25–30.
- [39] K. Rafiz, J.Y. Lin, Safe Li-ion batteries enabled by completely inorganic electrodecoated silicalite separators, Sustain. Energy Fuels 4 (2020) 5783–5794.
- [40] E.M. Flanigen, J.M. Bennett, R.W. Grose, J.P. Cohen, R.L. Patton, R.M. Kirchner, J. V. Smith, Silicalite, a new hydrophobic crystalline silica molecular sieve, Nature 271 (1978) 512–516.
- [41] M. Yu, J.L. Falconer, R.D. Noble, Adsorption of liquid mixtures on silicalite-1 zeolite: a density-bottle method, Langmuir 21 (2005) 7390–7397.
- [42] X. Lu, Y. Peng, Z. Wang, Y. Yan, A facile fabrication of highly b-oriented MFI zeolite films in the TEOS-TPAOH-H2O system without additives, Microporous Mesoporous Mater. 230 (2016) 49–57, https://doi.org/10.1016/j. micromeso.2016.04.037.
- [43] S. Ergun, Determination of particle density of crushed porous solids, Anal. Chem. 23 (1951) 151–156.
- [44] M.M. Treacy, J.B. Higgins, R. Ballmoos, Collection of Simulated XRD Powder Patterns for Zeolites, Elsevier, New York, 1996.
- [45] F. Banihashemi, A.F. Ibrahim, A.A. Babaluo, J.Y. Lin, Template-free synthesis of highly b-oriented MFI-type zeolite thin films by seeded secondary growth, Angew. Chem. Int. Ed. 58 (2019) 2519–2523.
- [46] M.G. Ahunbay, Monte Carlo simulation of water adsorption in hydrophobic MFI zeolites with hydrophilic sites, Langmuir 27 (2011) 4986–4993.
- [47] J. Landesfeind, J. Hattendorff, A. Ehrl, W.A. Wall, H.A. Gasteiger, Tortuosity determination of battery electrodes and separators by impedance spectroscopy, J. Electrochem. Soc. 163 (2016) 1373.
- [48] S.J. Todrigues, N. Vorhauer-Huget, T. Richter, E. Tsotsas, Influence of particle shape on tortuosity of non-spherical particle packed beds, Processes 11 (2022) 3.
- [49] X. Dong, W. Mi, L. Yu, Y. Jin, Y.S. Lin, Zeolite coated polypropylene separators with tunable surface properties for lithium-ion batteries, Microporous Mesoporous Mater. 226 (2016) 406–414.
- [50] M.Y. Wang, S.H. Han, Z.S. Chao, S.Y. Li, B. Tan, J.X. Lai, J.C. Fan, Celgard-supported LiX zeolite membrane as ion-permselective separator in lithium sulfur battery, J. Membr. Sci. 611 (2020), 118386.

- [51] K. Rafiz, D.R.L. Murali, J.Y. Lin, Suppressing lithium dendrite growth on lithiumion/metal batteries by a tortuously porous γ-alumina separator, Electrochim. Acta 421 (2022), 140478.
- [52] J. Liu, H. Yuan, X.-B. Cheng, W.-J. Chen, M.-M. Titirici, J.-Q. Huang, T.-Q. Yuan, Q. Zhang, A review of naturally derived nanostructured materials for safe lithium metal batteries, Materials Today Nano 8 (2019), 100049.
- [53] A. Varzi, K. Thanner, R. Scipioni, D. Di Lecce, J. Hassoun, S. Dörfler, H. Altheus, S. Kaskel, C. Prehal, S.A. Freunberger, Current status and future perspectives of lithium metal batteries, J. Power Sources 480 (2020), 228803.
- [54] H. Maleki, J.N. Howard, Internal short circuit in Li-ion cells, J. Power Sources 191 (2009) 568–574.
- [55] J. Zhang, L. Yue, Q. Kong, Z. Liu, X. Zhou, C. Zhang, L. Chen, Sustainable, heat-resistant and flame-retardant cellulose-based composite separator for high-performance lithium ion battery, Sci. Rep. 4 (2014) 1–8.
- [56] H.-B. Han, S.-S. Zhou, D.-J. Zhang, S.-W. Feng, L.-F. Li, K. Liu, W.-F. Feng, J. Nie, H. Li, X.-J. Huang, Lithium bis (fluorosulfonyl) imide (LiFSI) as conducting salt for

- nonaqueous liquid electrolytes for lithium-ion batteries: physicochemical and electrochemical properties, J. Power Sources 196 (2011) 3623–3632.
- [57] E. Paillard, Q. Zhou, W.A. Henderson, G.B. Appetecchi, M. Montanino, S. Passerini, Electrochemical and physicochemical properties of PY14FSI-based electrolytes with LiFSI, J. Electrochem. Soc. 156 (2009) A891.
- [58] D. Reber, R. Figi, R.-S. Kuehnel, C. Battaglia, Stability of aqueous electrolytes based on LiFSI and NaFSI, Electrochim. Acta 321 (2019), 134644.
- [59] W. Lin, M. Zhu, Y. Fan, H. Wang, G. Tao, M. Ding, N. Liu, H. Yang, J. Wu, J. Fang, Low temperature lithium-ion batteries electrolytes: rational design, advancements, and future perspectives, J. Alloys Compd. (2022), 164163.
- [60] S.S. Zhang, K. Xu, T.R. Jow, Electrochemical impedance study on the low temperature of Li-ion batteries, Electrochim. Acta 49 (2004) 1057–1061.
- [61] J. Dong, Y.S. Lin, M.Z.-C. Hu, R.A. Peascoe, E.A. Payzant, Template-removalassociated microstructural development of porous-ceramic-supported MFI zeolite membranes, Microporous Mesoporous Mater. 34 (2000) 241–253.